www.czasopisma.pan.pl PAN POLSKA AKADEMIA NAUK www.journals.pan.pl

PAN POLSKA AKADEMIA NAUK

JOURNAL OF WATER AND LAND DEVELOPMENT

e-ISSN 2083-4535

ITP-PIB

Polish Academy of Sciences (PAN) Institute of Technology and Life Sciences – National Research Institute (ITP – PIB)

JOURNAL OF WATER AND LAND DEVELOPMENT
DOI: 10.24425/jwld.2022.140377
2022, No. 52 (I–III): 87–94

Non-prismatic channels for reducing shear stress

Samir Haddad

Houari Boumediène University of Sciences and Technology, Faculty of Civil Engineering. LEGHYD Laboratory, BP 32 Bab Ezzouar, 16111 Algiers, Algeria

Akli Mohand Oulhadj University of Bouira, Rue Frères Boussendalah, 10000 Bouira, Algeria

RECEIVED 09.04.2021 REVIEWED 29.05.2021 ACCEPTED 08.09.2021

Abstract: To reduce the sediment transport capacity, shear stress needs to be reduced as well. The article describes work that has been done to find a way to make these reductions possible. The theoretical study and the approach proposed allowed us to obtain a general equation that determines conditions and calculates the most important parameters which support the reduction of shear stress. This describes the mechanism that erodes soils by free surface water flow.

In a similar vein, we have shown that adding a short non-prismatic channel to the entrance of a prismatic channel, which has the same geometric shape, is a very powerful way to reduce shear stress. With the idea of reducing shear stress, we have shown that the water-surface profile type plays a key role and must therefore be included in future reflections on reducing the importance of shear stress.

Additionally, the notion of efficiency was introduced that allows to evaluate the expected gain after the reduction of shear stress and adding a short non-prismatic channel.

The laws of similarity applied to free surface flows allowed us to obtain an equation with several equivalence scales and compare different geometric shapes in terms of their efficiency in the reduction of shear stress.

Keywords: detachment, non-prismatic channel, shear stress, soil erosion, transport capacity

INTRODUCTION

Regardless the nature of the channel, water loss by infiltration and evaporation is inevitable. In large channels, seepage loss can be up to 80% [Trout, Neibling 1993].

At the upstream end of the channel, the detachment rate is the highest because the flow is still high and the sediment concentration is low. The less the fluid is loaded with sediment, the more its erosive powers are. The detachment rate decreases along the channel because the its capacity decreases as well. This detail leads us to think that any project aimed at reducing the detachment of solid particles must be carried out in the upstream zone of the channel, which is located in the first quarters, or one thirds of its length.

Since the works by A. Brahms (1753), R.G. Kennedy (1895), G. Lacey (1930), E.W. Lane (1953), S. Leliavsky (1955), Th. Blench (1957) and C.R. Thorne (1998) were published and up to the present day, the search for stable channels with regard to erosion has remained relevant.

Smerdon and Beasley [1959] for cohesive soils and Lane [1953; 1955] for coarse soils have confirmed that the shear stress method is a good approach to studies to find erosion resistant channels. The scientific community calls these stable channels. In relation to their broad field of use, the search for stable channels aimed to define scientific and economic interests.

Chow [1959] demonstrated that channel erosion is a shear stress problem that varies along the wetted perimeter of the channel. Hence, we see that if we want channels to be stable and efficient, with respect to detachment, we must find means of reducing shear stress. Our idea is to add a non-prismatic channel at the entrance of the prismatic channel, which can be convergent or divergent. The main task of the non-prismatic channel is to reduce the erosive shear stress responsible for the detachment of soil particles during free surface flow inside the channels. This can be done by modifying channel's geometry.

Although the bibliography includes many examples of research into the ideal geometric shape of channels, it is impossible to determine a general and unified approach. The idea proposed, consisting in reducing shear stress by using non-prismatic channels, is original and no bibliographic references can be found.

STUDY METHODS

THEORETICAL BASIS

Once sediment is detached, it is transported by the flow for some distance primarily depending on aggregate size and density, and the transport capacity of the flow. Sediment is moved both as bed load and as suspended load. The transport capacity varies along the channel with the 3/2 power of shear stress. Trout and Neibling [1993] showed that the net erosion, which is equal to the detachment minus the deposit, is proportional to the difference between the sediment transport capacity and the sediment load, and it decreases as the sediment load increases. In addition, the carrying capacity of the channel is approached asymptotically rather than linearly.

Although the erosion capacity decreases along the channel in a similar fashion to the flow, the net erosion decreases more rapidly due to the increased sediment load that reaches the carrying capacity at the point where the residual flow is about 40% of the inlet flow. Beyond this point, which is approximately in the upper quarter or upper third of the channel, net erosion ends and net deposition begins [Trout, Neibling 1993].

Channels, without coating, are always more permeable than those coated by plastic, stones or cement. The degree of permeability depends on the geometric shape and on the characteristics of soil in which the channel is buried.

Precisely, because of the permeability, the flow passing through the initial channel (Q_i) is always reduced by one part, called the infiltrated flow (Q_{inf}) or lost (DQ), before arriving at the other channel (S_f) located at a distance L (Fig. 1). In other words:

$$Q_f = Q_i - Q_{\text{inf}} \tag{1}$$

According to the work of Moritz [Kraatz 1977] on the flows in the permeable channels, we can write:

$$Q_{\text{inf}} = C_0 L\sqrt{S} \tag{2}$$

$Q_f = Q_i - C_0 L\sqrt{S} = Q_i - \Delta Q$ or else:

$$\Delta Q = Q_f - Q_i = C_0 L\sqrt{S} \tag{3}$$

Assuming that:

$$Q_f = \beta Q_i \tag{4}$$

We will have:

$$Q_{\text{inf}} = (1-\beta)Q_i \tag{5}$$

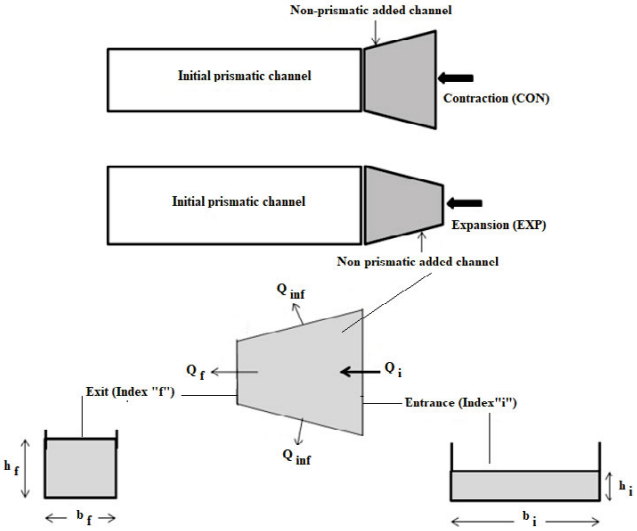

Fig. 1. Location and geometry of added non-prismatic channels; source: own elaboration

From the previous equations, we can write: $\beta Q_i = Q_i - C_0 L\sqrt{S}$ $\Rightarrow \beta = \left[1 - \frac{C_0 L\sqrt{S}}{Q_i}\right] < 1$

At the entry of the small non-prismatic channel or singularity, index *i*, the shear stress is:

$$\tau_i = (\rho g R_H)_i \tag{6}$$

At the end of the same singularity, index *f*, the shear stress is:

$$\tau_f = (\rho g R_H)_f \tag{7}$$

So:

$$\frac{\tau_i}{\tau_f} = \frac{(R_H)_i}{(R_H)_f}\frac{I_i}{I_f} \tag{8}$$

Knowing that:

$$V = \frac{R_H^{2/3}\sqrt{I}}{n} = \frac{Q}{S} \tag{9}$$

$$R_H = \frac{S}{P} \tag{10}$$

We can write:

$$I = \frac{n^2 Q^2 P^{4/3}}{S^{10/3}} \tag{11}$$

Finally:

$$\frac{\tau_i}{\tau_f} = \left(\frac{Q_i}{Q_f}\right)^2 \left(\frac{P_i}{P_f}\right)^{1/3} \left(\frac{S_f}{S_i}\right)^{7/3} \tag{12}$$

Therefore, for the hydraulic (bed) shear stress to decrease, it is necessary that:

$$\frac{\tau_i}{\tau_f} > 1 \tag{13}$$

So, $\left(\frac{Q_i}{Q_f}\right)^2\left(\frac{P_i}{P_f}\right)^{1/3}\left(\frac{S_f}{S_i}\right)^{7/3} > 1$. With, $\beta = Q_i/Q_f$, $P^* = P_i/P_f$ and $S^* = S_i/S_f$, we can write:

$$\beta^2 \frac{P^{*1/3}}{S^{*7/3}} > 1 \tag{14}$$

This is the general shear stress reduction equation.

We are going to apply this expression to different geometric shapes: trapezoid (TPZ), rectangle (REC), triangle (TRG) and semicircle (CIR).

REDUCTION OF SHEAR STRESS BY GEOMETRICAL SHAPES

Trapezoidal form (TPZ)

To simplify the study and design of channels of a trapezoidal cross section, slopes of embankments $m_i = n_i = m_f = n_f = m$, remain constant (Fig. 2).

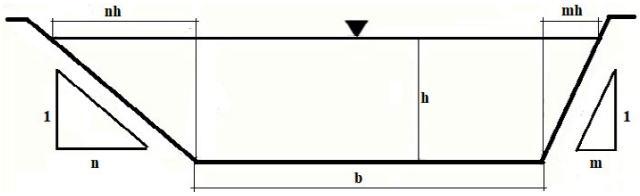

Fig. 2. Shape of the general trapezoidal cross-channel; source: own elaboration

At the entry of the channel:

$$P_i = b_i + 2h_i\sqrt{1+m^2} \text{ and } S_i = h_i b_i + h_i^2 m \tag{15}$$

At the exit of the channel:

$$P_f = b_f + 2h_f\sqrt{1+m^2} \text{ and } S_f = h_f b_f + h_f^2 m \tag{16}$$

By applying the general shear stress reduction equation (Eq. 14), we will have:

$$\beta^2 \frac{\left(\frac{b_i + 2h_i\sqrt{1+m^2}}{b_f + 2h_f\sqrt{1+m^2}}\right)^{1/3}}{\left(\frac{h_i b_i + h_i^2 m}{h_f b_f + h_f^2 m}\right)^{7/3}} > 1 \tag{17}$$

With, $\beta = Q_i/Q_f$, $S^* = S_i/S_f$ and $P^* = P_i/P_f$, we can write:

$$\beta^2 \frac{P^{*1/3}}{S^{*7/3}} > 1 \tag{18}$$

Therefore, for the shear stress to decrease, it suffices to check the above inequality.

Rectangular form (REC)

Just take the established expression for the trapezoid (Eq. 17) and set $m_i = m_f = m = 0$, this gives:

$$\beta^2 \frac{\left(\frac{b_i + 2h_i}{b_f + 2h_f}\right)^{1/3}}{\left(\frac{h_i b_i}{h_f b_f}\right)^{7/3}} > 1 \tag{19}$$

With, $\beta = Q_i/Q_f$, $\alpha = b_i/b_f$, $P^* = P_i/P_f$ and $\varphi = h_i/h_f$, we can write:

$$\beta^2 \frac{P^{*1/3}}{\alpha^{7/3}\varphi^{7/3}} > 1 \tag{20}$$

Therefore, for the shear stress to decrease, it suffices to check the last inequality.

Triangular form (TRG)

Just take the established expression for the trapezoid (Eq. 17) and set $n_i = m_i = v_i$, $n_f = m_f = v_f$, $b_i = b_f = 0$, $\beta = Q_i/Q_f$, $\varphi = h_i/h_f$ and v_i, v_f are angles of the curved walls of the triangular channel at the entrance and exit (Fig. 3), this gives:

$$\beta^{12} \frac{\left(1 + v_i^2\right)v_f^{14}}{\left(1 + v_f^2\right)v_i^{14}\varphi^{26}} > 1 \tag{21}$$

Finally, for the shear stress to decrease, it suffices to check the above inequality.

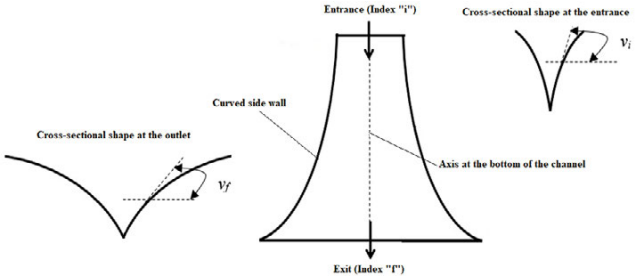

Fig. 3. Added non-prismatic triangular channel geometry; source: own elaboration

Circular form (CIR)

At the entrance to the channel (Fig. 4), we have:

$$P_i = R_i\theta_i \text{ and } S_i = 0.5R_i^2(\theta_i - \sin\theta_i) \tag{22}$$

At the exit of the channel, we have:

$$P_f = R_f\theta_f \text{ and } S_f = 0.5R_f^2(\theta_f - \sin\theta_f) \tag{23}$$

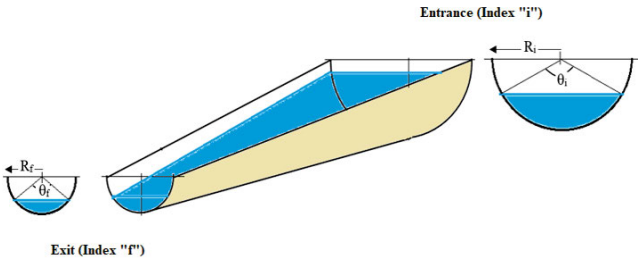

Fig. 4. Flow through a convergent (Contraction, CON) non-prismatic circular channel (CIR); source: own elaboration

For the same above condition (Eq. 14), we have:

$$\frac{\tau_i}{\tau_f} = \frac{\frac{Q_i^2(R_i\theta_i)^{1/3}}{\left[0.5R_i^2(\theta_i - \sin\theta_i)\right]^{7/3}}}{\frac{Q_f^2\left(R_f\theta_f\right)^{1/3}}{\left[0.5R_f^2\left(\theta_f - \sin\theta_f\right)\right]^{7/3}}} > 1 \tag{24}$$

Mathematically, we can find that:

$$(\theta - \sin\theta) \approx 0.1454\,\theta^{\,2.8345} \tag{25}$$

With correlation coefficient, r = 0.9992.
So, with, $\beta = Q_i/Q_f, \lambda = \theta_i/\theta_f$ and $\chi = R_i/R_f$, we can write:

$$\beta^2 \frac{1}{\chi^{4.333}\lambda^{6.281}} > 1 \tag{26}$$

Then, to reduce the shear stress in circular channels, it is necessary to check the above inequality.

EFFECTIVENESS IN REDUCING SHEAR STRESS

We introduce the concept of efficiency (ψ) which reflects the rate of reduction of shear stress while passing from a cross channel to another, over a certain length, under the exclusive effect of a plain change of its geometry. In other words, the efficiency provides information on the gain in reducing shear stress, which can be obtained by adding converging (CON) or diverging (EXP) non-prismatic channels (Fig. 5) at the entry of the prismatic channels (PRI). This addition, if it proves to be effective in reducing the shear stress, can be considered as a device for stabilising the soil with respect to detachment.

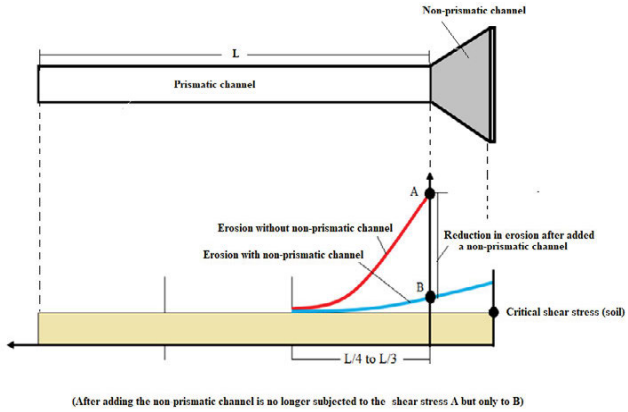

Fig. 5. The effect of adding a non-prismatic channel to reduce shear stress; source: own elaboration

By definition, the efficiency of the reduction of the shear stress is:

$$\psi = \frac{\tau_i - \tau_f}{\tau_i} = 1 - \frac{\tau_f}{\tau_i} \tag{27}$$

Calculation of the efficiency for the trapezoidal (TPZ) shape

From Equation (27), we have:

$$\psi_{TPZ} = 1 - \frac{\tau_f}{\tau_i} = \frac{\frac{P_f}{S_f^7}}{\beta^6\frac{P_i}{S_i^7}} = 1 - \frac{\frac{b_f + 2h_f\sqrt{1+m^2}}{\left(h_f b_f + h_f^2 m\right)^7}}{\beta^6\frac{b_i + 2h_i\sqrt{1+m^2}}{\left(h_i b_i + h_i^2 m\right)^7}} \tag{28}$$

If $m_i = m_f = m$, $\beta = Q_i/Q_f$, $P^* = P_i/P_f$ and $R_H^* = \frac{R_{H_i}}{R_{H_f}}$, then:

$$\psi_{TPZ} = 1 - \frac{S^{*7/3}}{\beta^2 P^{*1/3}} \tag{29}$$

From the above expression, to maximise ψ_{TPZ} we have to minimise $(\frac{S^{*7/3}}{\beta^2 P^{*1/3}})$

A mathematical analysis allows establishing the results below.

$$\psi_{TPZ} = \max \Leftrightarrow \frac{S^{*7/3}}{\beta^2 P^{*1/3}} = \min \Leftrightarrow \begin{cases} \alpha > 1 \text{ (CON)} \\ \varphi < 1 \text{ (M1, M3, S1, S3)} \end{cases}$$

Comment. In trapezoidal channels, the addition of converging (CON) channels maximises the efficiency of reducing shear stress. The water surface profile must be of the M1, M3, S1 or S3 type (Figs. 6–9). However, the M1 and S1 water-surface profile types are preferred because the differences in water depth between the inlet and the outlet of the non-prismatic channel are greater than those that can be obtained with the M3 and S3 water-surface profile types.

Finally, note that inside a non-prismatic channel, it is possible to have a change in the water-surface profile, which can pass from M1 to S1 or from S1 to M1. In other words, inside the non-prismatic channel, the flow can shift from supercritical (Fr > 1) to subcritical (Fr < 1) and vice-versa. Indeed, the "S" water-surface profile type appears as soon as the critical height (H_C) exceeds the normal depth (H_N). For the "M" water-surface profile type, it is exactly the opposite. Since H_C and H_N are a function of the length of the non-prismatic section, it is very likely that there is a critical length (L_C) for which $H_C = H_N$. Exceeding L_C, H_C is no longer greater than H_N, but, on the contrary, H_C will become less than H_N. To avoid this change of water-surface profile, it is necessary to have $H_C > H_N$ all the time to guarantee an "S" water-surface profile type and $H_N > H_C$ to guarantee an "M" water-surface profile type.

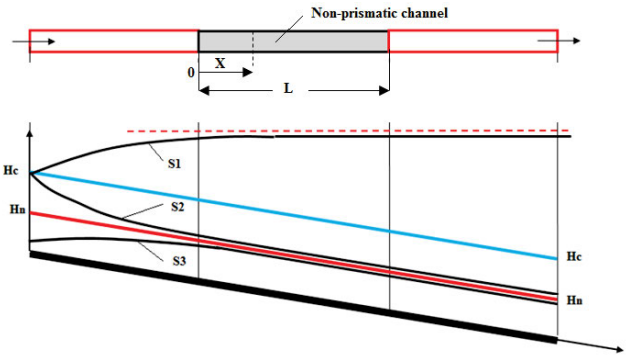

Fig. 6. Water-surface profile type "S" for prismatic channel; source: own elaboration

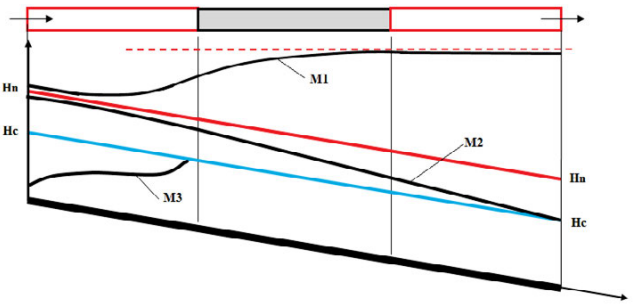

Fig. 7. Water-surface profile type "M" for prismatic channel; source: own elaboration

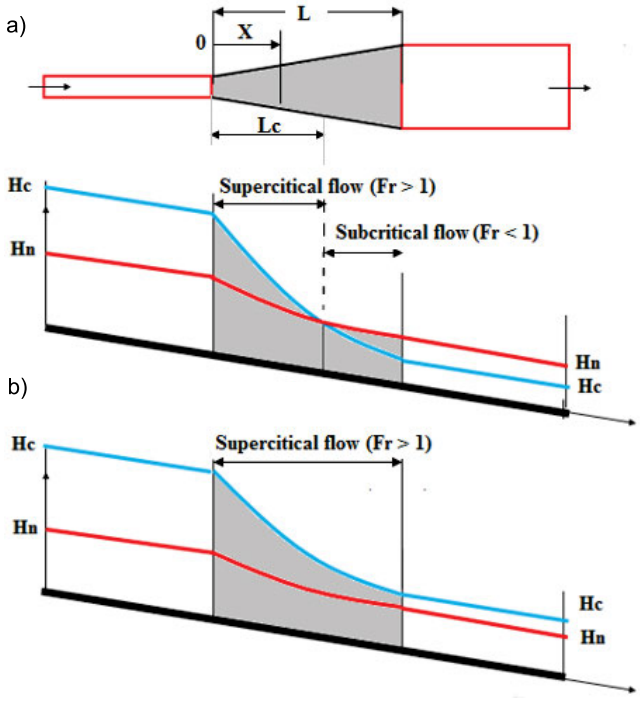

Fig. 8. Water-surface profile type "S" for non-prismatic channel (Expansion, EXP): a) with change in flow regime, b) without change in flow regime; source: own elaboration

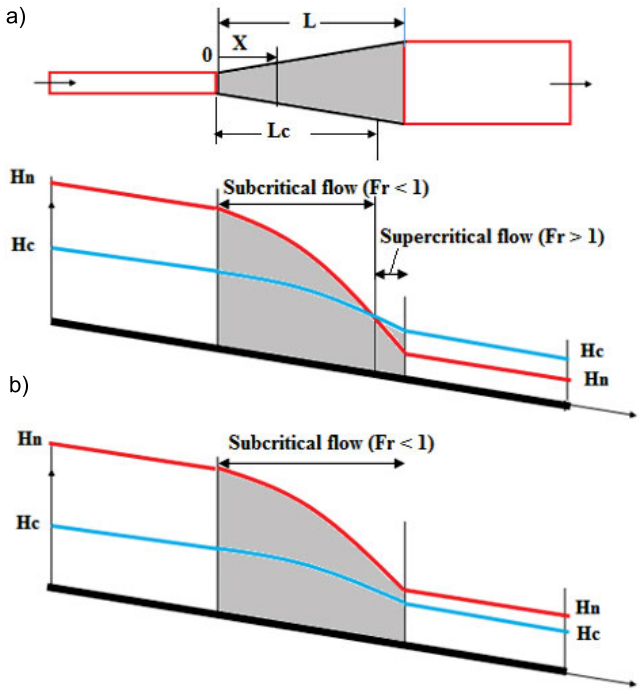

Fig. 9. Water-surface profile type "M" for non-prismatic channel (Expansion, EXP): a) with change in flow regime, b) without change in flow regime; source: own elaboration

This kind of problem was initially discussed by Poincaré [1881] and then developed by Massé [1938].

Before moving onto the calculations, it is important to remember that the adoption of a flow regime, i.e. supercritical flow (Fr > 1 and $H_C > H_N$) inside the channel, will create an oblique hydraulic jump.

Mathematically, critical depth (H_C) is obtained after solving the equation:

$$\mathrm{Fr} = 1 \Leftrightarrow \mathrm{Fr} = \frac{\sqrt{B}\left(1 + I_0^2\right)^{1/4}\sigma Q}{\sqrt{S^3}\sqrt{g}} = 1 \Rightarrow \frac{S^3}{B} = \frac{Q^2\sigma^2\sqrt{1 + I_0^2}}{g} \quad (30)$$

where: Fr = Froude number, B = top width which is a function of X, S = wetted surface which is a function of X, σ = energy (Coriolis) coefficient, I_0 = longitudinal slope of the channel (bed slope), Q = flow rate.

Solving the above equation will give the critical depth (H_C) not fixed, but varying with the length of the channel.

To obtain the normal depth (H_N), we must solve the Chézy equation with $I = I_0$:

$$V = \frac{R_H^{2/3}\sqrt{I_0}}{n} = \frac{Q}{S} \quad (31)$$

$$R_H = \frac{S}{P} \quad (32)$$

$$\frac{S^{5/2}}{P} = \left(\frac{n^2Q^2}{I_0}\right)^{3/4} \quad (33)$$

where: n = Manning's coefficient of the channel's roughness, P = wetted perimeter which is a function of X, S = wetted surface which is a function of X, I_0 = longitudinal slope of the channel (bed slope), Q = flow rate.

Solving the above equation will make normal depth (H_N) not fixed but varying with the length of the channel.

Finally, to have the water-surface profile type S1, it is necessary that the critical depth (H_C) obtained from Equation (30) is greater than the normal depth (H_N) obtained from Equation (33). In the same way, to have the water-surface profile type M1, it is necessary that the critical depth (H_C) obtained from Equation (30) is less than the normal depth (H_N) obtained from Equation (33).

Due to infiltration through the channels, β is always greater than one and this further increases the efficiency.

Calculation of the efficiency for the rectangular (REC) shape

From Equations (27) and (28) and for $m = 0$, we have:

$$\psi_{\mathrm{REC}} = 1 - \frac{\tau_f}{\tau_i} = \frac{\frac{P_f}{S_f^t}}{\beta^6\frac{P_i}{S_i^t}} = 1 - \frac{\frac{b_f + 2h_f}{\left(h_f b_f\right)^7}}{\beta^6\frac{b_i + 2h_i}{\left(h_i b_i\right)^7}}$$

If, $\beta = Q_i/Q_f$, $R_H^* = \frac{R_{H_i}}{R_{H_f}}$, $\alpha = b_i/b_f$ and $\varphi = h_i/h_f$, then:

$$\psi_{\mathrm{REC}} = 1 - \frac{\varphi^{7/3}\alpha^{7/3}}{\beta^2 P^{*1/3}} \quad (34)$$

From the above expression, to maximise ψ_{REC} we have to minimise $\frac{\varphi^{7/3}\alpha^{7/3}}{\beta^2 P^{*1/3}}$.

A mathematical analysis allows establishing the results below.

$$\psi_{\mathrm{REC}} = \max \Leftrightarrow \frac{\varphi^{7/3}\alpha^{7/3}}{\beta^2 P^{*1/3}} = \min \Leftrightarrow \alpha < 1(\mathrm{EXP})$$

Comment. The addition of divergent non-prismatic (EXP) channels maximises the efficiency in reducing shear stresses in rectangular shaped geometric channels. The water surface profile (Figs. 6 to 10) is not a decisive parameter. Due to infiltration through the wetted perimeter of the channels, β is always greater than one and this further increases the efficiency, but as with the trapezoidal geometric shape (TPZ), attention should be paid to oblique jumps.

Calculation of the efficiency for the triangular (TRG) shape

From Equations (14) and (21), we can write, $\frac{\tau_i}{\tau_f} = \beta^{12}\frac{\left(1+v_i^2\right)v_f^{14}}{\left(1+v_f^2\right)v_i^{14}\varphi^{26}}$

From Equation (27) and if, $\Omega = v_i/v_f$, $\beta = Q_i/Q_f$ and $\varphi = h_i/h_f$, then we can deduce that:

$$\psi_{\mathrm{TRG}} = 1 - \frac{\left(1 + v_f^2\right)\Omega^{14}\varphi^{26}}{\beta^{12}\left(1 + v_i^2\right)} \tag{35}$$

From the above expression, to maximise ψ_{TRG} we have to minimise $\frac{\left(1+v_f^2\right)\Omega^{14}\varphi^{26}}{\beta^{12}\left(1+v_i^2\right)}$

A mathematical analysis allows establishing the results below.

$$\psi_{\mathrm{TRG}} = \max \Leftrightarrow \frac{\left(1 + v_f^2\right)\Omega^{14}\varphi^{26}}{\beta^{12}\left(1 + v_i^2\right)} = \min \Leftrightarrow \begin{cases} \Omega < 1\ (\mathrm{EXP}) \\ \varphi < 1\ (\mathrm{M1,\ M3,\ S1,\ S3}) \end{cases}$$

Comment. In triangular channels, the addition of diverging (EXP) channels maximises the efficiency in reducing shear stress. The water surface profile must be of the M1, M3, S1 or S3 type (Figs. 6–10). However, the M1 and S1 water-surface profile types are preferred because differences in water depth between the inlet and the outlet, of the non-prismatic channel, are greater than those that can be obtained with the M3 and S3 water surface profiles.

Due to infiltration through the channels, β is always greater than one and this further increases the efficiency. We should point out that the use of the triangular shape is not recommended because the construction of non-prismatic sections, converging or diverging, is very difficult because sidewalls that are initially rectilinear become curved walls (Fig. 3).

Calculation of the efficiency for the circular (CIR) shape

From Equations (24) and (27), we have:

$$\psi_{\mathrm{CIR}} = 1 - \frac{\tau_f}{\tau_i} = \frac{\frac{P_f}{S_f^7}}{\beta^6\frac{P_i}{S_i^7}} = 1 - \frac{\frac{\left(R_f\theta_f\right)}{\left[0.5R_f^2\left(\theta_f - \sin\theta_f\right)\right]^7}}{\beta^6\frac{\left(R_i\theta_i\right)}{\left[0.5R_i^2\left(\theta_i - \sin\theta_i\right)\right]^7}}$$

If, $\beta = Q_i/Q_f$, $\lambda = q_i/q_f$ and $\chi = R_i/R_f$, we can write:

$$\psi_{\mathrm{CIR}} = 1 - \frac{\chi^{4.333}\lambda^{6.281}}{\beta^2} \tag{36}$$

From the above expression, to maximise ψ_{CIR} we have to minimise $\frac{\chi^{4.333}\lambda^{6.281}}{\beta^2}$.

A mathematical analysis allows establishing the results below.

$$\psi_{\mathrm{CIR}} = \max \Leftrightarrow \frac{\chi^{4.333}\lambda^{6.281}}{\beta^2} = \min \Leftrightarrow$$

$$\begin{cases} \chi > 1\ (\mathrm{CON}) \Leftrightarrow \begin{cases} \lambda > 1\ (\mathrm{M1,\ M3,\ }S1, S3) \\ \lambda < 1\ (\mathrm{M2,\ S2}) \end{cases} \\ \chi < 1\ (\mathrm{EXP}) \Leftrightarrow \lambda > 1\ (\mathrm{M1,\ M3,\ S1,\ S3}) \end{cases}$$

Comment. In circular channels, the addition of converging ($\chi > 1$) or diverging ($\chi < 1$) channels maximises the efficiency in reducing shear stress. To decide which of the two is more effective, we have to perform laboratory experiments.

However, the M1 and S1 water-surface profile types are preferred because differences in water depth between the inlet and the outlet, of the non-prismatic channel, are greater than those that can be obtained with the M3 and S3 water surface profiles (see commentary of section "Efficiency in the case of the trapeze (TPZ)" for the justification). Due to infiltration through the channels, b is always greater than one and this further increases the efficiency.

INFLUENCE OF CHANNEL GEOMETRY ON EFFICIENCY

It is interesting to know which of the four geometric shapes of the non-prismatic channels is the most efficient in reducing shear stress responsible for sediment detachment and transport problems.

To be able to make comparisons, between various geometrical forms, as regards the best reduction of shear stress, the laws of similarity of flows with free surface and sediment transport are used [Dey 2014; Ettema *et al.* (eds.) 2000; Haddad, Bouhadef 2019; Henderson 1966; Pugh 1985; Yalin 1971].

The study of the laws of similarity, by the application of the above conditions, made it possible to obtain the following equivalence scale:

$$K_S^{49} = K_P^{10}K_B^4 \tag{37}$$

This equivalence scale shows that the scale of the wetted area (K_S) to the power of forty-nine is equal to the scale of the wetted perimeter (K_P) to the power of ten multiplied by the scale of the upper width of the channels (K_B) to the power of four.

This scale allows the passage from one geometric shape to another while respecting the laws of similarity. This scale is very interesting because it allows to compare all the geometric shapes in terms of their efficiency in reducing shear stress and thus to determine the best shape.

RESULTS AND DISCUSSION

Based on the theoretical study, we can make the following remarks:

- in trapezoidal prismatic channels, to increase efficiency we add only non-prismatic converging channels (CON) and the water surface profile should be M1 with $H_N > H_C$ or S1 with $H_C > H_N$; for this last choice, one should pay attention to the oblique jumps that will appear;
- for rectangular prismatic channels, to increase efficiency we need to add non-prismatic divergent channels (EXP); the water surface profile is not a decisive parameter;

– in triangular prismatic channels, the addition of non-prismatic diverging channels increases the efficiency and the water surface profile should be M1 with $H_N > H_C$ or S1 with $H_C > H_N$; for this last choice, one should pay attention to the oblique jumps that will appear;
– in circular channels, the addition of converging ($\chi > 1$) or diverging ($\chi < 1$) channels maximises the efficiency of reducing shear stress; to decide which of the two is more effective, we have perform laboratory experiments.

As said previously, we must always favour the water-surface profile type M1 instead of M3 and S1 instead of S3. For this last choice, one should pay attention to the oblique jump that will appear.

All results of the efficiency study are given in Table 1.

Table 1. Summary of the results of the efficiency study

Shape	Contraction (CON)						Expansion (EXP)					
Geometrical form	M1	M2	M3	S1	S2	S3	M1	M2	M3	S1	S2	S3
Trapeze (TPZ)	X			X								
Rectangle (REC)							X	X	X	X	X	X
Triangle (TRG)							X			X		
Circle (CIR)	X	X		X	X		X			X		

Source: own study.

The Table 1 summarises all possibilities to improve the reduction of shear stress that depends on the geometric shape of the non-prismatic channel and the type of water-surface profile:
– for a trapezoidal channel (TPZ), you need a converging non-prismatic channel; the water-surface profile will be M1 and S1 type;
– for a rectangular channel (REC), you need a divergent non-prismatic channel; all types of water-surface profiles are possible;
– for a triangular channel (TRG), a divergent non-prismatic channel is needed; the water-surface profile will be M1 and S1 type;
– for a circular channel (CIR), you need a converging non-prismatic channel and water-surface profile will be M1, M2, S1 and S2 type; a divergent non-prismatic channel with M1 and S1 water-surface profile type further improves the efficiency.

CONCLUSIONS

In conclusion, it is believed that the proposed idea, which consists in adding a non-prismatic channel, contraction or expansion, at the entry of prismatic channels, is an interesting way to reduce shear stress responsible for soil detachment. In addition, we have shown that the efficiency in reducing shear stress is a function of water-surface profiles and the geometry of channels.

Finally, we have set up an equivalence scale, which makes it possible to compare the efficiency obtained by each type of non-prismatic channel geometry and to predict efficiencies for other soil, slope and flow cases without having to repeat the experiment.

This approach is a purely theoretical one. We think that it is essential to carry out experiments in order to validate the proposed method.

Before concluding, it is worth pointing out that we have already shown that the geometric shape of the prismatic channel strongly influences the dynamics of sediments. On this basis and with the proposed new approach, we believe that the combination of the two will further reduce soil erosion. In other words, to reduce soil erosion of channels, one can choose the geometric shape of a prismatic channel added at its entrance; we can add a non-prismatic channel of geometric shape similar to those of prismatic ones. With an appropriate choice of the water-surface profile, which depends on the subcritical or supercritical flow regime, we believe that the efficiency in reducing shear stress can be better.

ACKNOWLEDGMENTS

This study was carried out in the LEGHYD Laboratory of the Houari Boumediène University of Sciences and Technology (USTHB) without any external funding.

NOTATIONS

V (m·s^{-1})	average water velocity
Index i	entrance (entry channel)
Index f	exit (outlet channel)
τ (N·m^{-2})	shear stress
ρ (kg·m^{-3})	density of water
I (%)	energy slope
I_0 (%)	bed slope
n (s·m$^{-1/3}$)	Manning roughness coefficient
B (m)	width of the channel at the level of the free surface (top width)
b (m)	width of the channel at the base (bed width)
S (m^2)	wetted area
P (m)	wetted perimeter
R_H (m) = S/P	hydraulic radius
g (m·s^{-2})	gravitational acceleration
Q (m^3·s^{-1})	discharge
$Q_{inf} = \Delta Q$ (m^3·s^{-1})	infiltration flow through the walls and the base of the channel
C_0	experimental coefficient which depends on the type of soil
L (m)	length of the channel from the inlet (entrance) and the outlet (exit)
σ	energy coefficient = Coriolis coefficient
$\beta = Q_i/Q_f$	ratio of discharges

$\lambda = q_i/q_f$	ratio of angles of water depth in a semi-circular channel
$\psi = 1 - t_f/t_i$	efficiency
$\varphi = h_i/h_f$	ratio of water depth
$\chi = R_i/R_f$	ratio of radius in semicircular channel
if $\chi < 1$	expansion circular channel (EXP)
if $\chi = 1$	prismatic circular channel (PRI)
if $\chi > 1$	contraction circular channel (CON)
$\Omega = v_i/v_f$	ratio of wall angles in triangular channel
if $\Omega < 1$	expansion triangular channel (EXP)
if $\Omega = 1$	prismatic triangular channel (PRI)
if $\Omega > 1$	contraction triangular channel (CON)
$\alpha = b_i/b_f$	ratio of bed widths
if $\alpha < 1$	expansion rectangular and trapezoidal channel (EXP)
if $\alpha = 1$	prismatic rectangular and trapezoidal channel (PRI)
if $\alpha > 1$	contraction rectangular and trapezoidal channel (CON)
$\mathrm{Fr} = \frac{\sqrt{B}\left(1+I_0^2\right)^{1/4}\sigma Q}{\sqrt{S^3}\sqrt{g}}$	Froude number

REFERENCES

Beczek M., Ryżak M., Sochan A., Mazur R., Polakowski C., Hess D., Bieganowski A. 2020. Methodological aspects of using high-speed cameras to quantify soil splash phenomenon. Geoderma. Vol. 378, 14592. DOI 10.1016/j.geoderma.2020.114592.

Chaudhry M.H. 2008. Open-channel flow. 2nd ed. Springer Science + Business Media, LLC, New York, USA. ISBN 978-0-387-30174-7 pp. 523.

Chow V.T. 1959. Open channel hydraulics. McGraw Hill. ISBN 07-010776-9 pp. 702.

Dey S. 2014. Fluvial hydrodynamics. Ser. GeoPlanet: Earth and Planetary Sciences. Berlin, Germany. Springer-Verl. ISBN 978-3642190612 pp. 719.

Ettema R. 2000. Hydraulic modeling. Concepts and practices. ASCE Manuals and Reports on Engineering Practice. No. 97. ISBN 978-0784404157 pp. 390.

Haddad S., Bouhadef M. 2019. Contribution à l'étude du phénomène de transport des sédiments par érosion des sols [Contribution to the study of the phenomenon of sediment transport by soil erosion] [online]. PhD Thesis. Algiers, Algeria. USTHB pp. 136. [Access 10.02.2021]. Available at: http://repository.usthb.dz//xmlui/handle/123456789/8210

Haddad S., Bouhadef M. 2018. Contribution to runoff erosion of earthen channels. Polish Journal of Soil Science. Vol. 51. No. 2 p. 313–325. DOI 10.17951/pjss.2018.51.2.313.

Henderson F.M. 1966. Open channel flow. New York, USA. MacMillan Company. ISBN 978-0023535109 pp. 522.

Kraatz D.B. 1977. Irrigation channel lining. FAO. Italy. ISBN 9251001650 pp. 199.

Lane E.W. 1953. Progress report on studies on the design of stable channels. Bureau of Reclamation. Proceedings. No. 79. New York, USA. ASIN B0007I585M pp. 31.

Lane E.W. 1955. Design of stable alluvial channels. Transactions of the American Society of Civil Engineers. Vol. 120. Iss. 1 p. 1234–1260.

Massé P. 1938. Ressaut et ligne d'eau dans les cours d'eau à pente variable [Hydraulic jump and flow profile in channels of variable slope]. Revue Générale de l'Hydraulique. Vol. 4. No. 19 p. 7–11.

Poincaré H. 1881. Mémoires sur les courbes définies par une équation différentielle [Memoir on the curves defined by a differential equation] [online]. Journal de Mathématiques Pures et Appliquées. Ser. 3. Vol. 7 p. 375–422. [Access 10.02.2021]. Available at: http://sites.mathdoc.fr/JMPA/PDF/JMPA_1881_3_7_A20_0.pdf

Pugh C.A. 1985. Hydraulic model studies of fuse plug embankments [online]. Denver, CO. Bureau of Reclamation, Engineering and Research Center. Report No. REC-ERC-85-7 pp. 33. [Access 20.02.2021]. Available at: https://www.usbr.gov/tsc/techreferences/rec/REC-ERC-85-7.pdf

Smerdon E.T, Beasley R.P. 1959. The tractive force theory applied to stability of open channels in cohesive soils [online]. Columbia, MO. University of Missouri, Missouri. USA. Agricultural Experiment Station. Research Bulletin. No. 715 pp. 36. [Access 20.02.2021]. Available at: https://mospace.umsystem.edu/xmlui/handle/10355/58141

Trout T.J., Neibling W.H. 1993. Erosion and sedimentation processes on irrigated fields. Journal of Irrigation and Drainage Engineering. Vol. 119. No. 6. DOI 10.1061/(ASCE)0733-9437(1993)119:6(947).

Yalin M.S. 1971. Theory of hydraulic models. London. Macmillan Civil Engineering Hydraulics. The Macmillan Press LTD, USA. ISBN 978-0408004824 pp. 266.